

Available online at www.sciencedirect.com

Physics Procedia 3 (2010) 1295–1298

**Physics
Procedia**

www.elsevier.com/locate/procedia

Semimetallic properties of SnTe/PbSe type-II superlattices

Akihiro Ishida¹, Tomohiro Yamada¹, Takuro Tsuchiya¹, Yoku Inoue¹, and Takuji Kita²

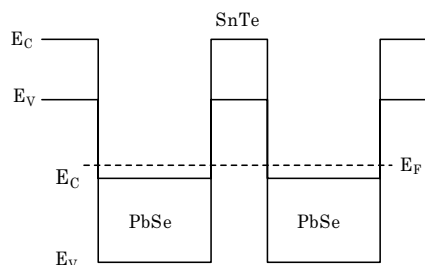
1.- Department of Electrical and Electronic Engineering, Shizuoka University, Johoku 3-5-1, Hamamatsu 432-8561, Japan; e-mail: tdaishi@ipc.shizuoka.ac.jp

2.- TOYOTA Motor Co. Mishuku 1200, Susono 410-1193, Japan

We prepared the SnTe/PbSe superlattices, and measured electrical and optical properties at room temperature. The superlattice showed semimetallic properties resulting from type-II band offset between SnTe and PbSe. Though nondope SnTe had hole concentration around $3 \times 10^{20} \text{cm}^{-3}$, nondope SnTe/PbSe superlattices with thin SnTe layers showed n-type conduction with carrier concentrations less than $2 \times 10^{18} \text{cm}^{-3}$ and carrier mobility comparable or higher than that of PbSe, keeping semimetallic properties in the optical transmission spectra. These properties are discussed with the band offset of SnTe/PbSe heterojunction.

1. Introduction

The IV-VI compound semiconductors and quantum wells have various applications such as infrared detectors, lasers, and thermoelectric devices. Among the IV-VI materials lead chalcogenides have been studied extensively, owing to the facility to control carrier concentration. On the other hand, the SnTe normally indicates p-type conduction with the carrier concentration of the order of 10^{20}cm^{-3} .¹ It is expected that the superlattice combined with the SnTe and lead chalcogenide indicates interesting electrical properties due to the special band offset. We proposed PbTe/SnTe heterojunction becomes type-II where valence band top is higher than the conduction band bottom of PbTe,^{2,4} and confirmed that the PbTe/SnTe superlattice has semimetallic properties. Similar band offset is expected for SnTe/PbSe system. Figure 1 shows the expected band offset of the SnTe/PbSe heterojunction. In the superlattice, carriers in the SnTe valence band flow into the conduction band of the PbSe, and semimetallic properties should appear. In this



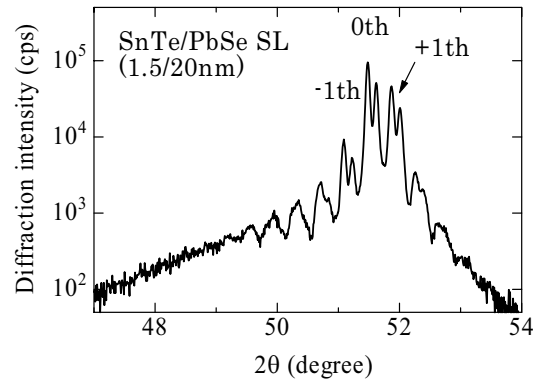
paper, we describe electrical and optical properties of the SnTe/PbSe superlattices.

Fig.1. Schematic band diagram of the SnTe/PbSe superlattice.

2. Experimental

The SnTe/PbSe superlattices were prepared by hot wall epitaxy directly on $\text{BaF}_2(111)$ substrates.⁵ Fig. 2 shows the x-ray diffraction pattern of SnTe/PbSe (1.5/20nm) superlattice.

Many satellites were observed, showing good periodicity and small interdiffusion of the constituents. To prepare SnTe/PbSe superlattices, 5N stoichiometric SnTe and PbSe polycrystals were used as the source materials. Carrier types of the films prepared from the source materials were all p-type. Carrier concentrations of PbSe were of the order of 10^{17} cm^{-3} , and those of SnTe were of the order of 10^{20} cm^{-3} . Table I shows the electrical properties of the SnTe, PbSe films and SnTe/PbSe superlattices at



room temperature. The SnTe/PbSe superlattice with thin SnTe layer indicated n-type conduction as expected, even though both SnTe and PbSe had p-type conduction. Similar property has been observed for PbTe/SnTe superlattices.⁶ These properties come from the type-II band structure. Figure 3 shows a schematic L-point subband structure for the superlattice. In the (111) growth, real subband structures are more complicated because there are two kinds of subbands corresponding to the valley with superlattice direction and other $\langle 111 \rangle$ valleys oblique to the superlattice direction. Similar property has been observed for

Fig.2 X-ray diffraction pattern of a SnTe/PbSe SL

Table I Electrical properties of SnTe, PbSe, and SnTe/PbSe superlattices.

Sample	Structure	Resistivity	Mobility	P/N	Carrier
		(Ωcm)	(cm^2/Vs)		Concentration
					(cm^{-3})
SnTe	$1.7\mu\text{m}$	0.00015	200	p	2.0×10^{20}
PbSe	$1.7\mu\text{m}$	0.033	530	p	3.5×10^{17}
SnTe/PbSe SL	(10-10nm)*100	0.0029	6	n	3.3×10^{20}
SnTe/PbSe SL	(10-10nm)*100	0.003	34	p	6.1×10^{19}
SnTe/PbSe SL	(20-20nm)*100	0.0031	110	p	1.9×10^{19}
SnTe/PbSe SL	(20-20nm)*100	0.0051	72	p	1.7×10^{19}
SnTe/PbSe SL	(10-20nm)*100	0.005	250	n	5.1×10^{18}
SnTe/PbSe SL	(10-30nm)*50	0.0026	480	n	5.1×10^{18}
SnTe/PbSe SL	(5-20nm)*100	0.011	230	n	2.6×10^{18}
SnTe/PbSe SL	(2.5-20nm)*100	0.0095	130	n	5.0×10^{18}
SnTe/PbSe SL	(2.5-30nm)*100	0.0065	560	n	1.7×10^{18}
SnTe/PbSe SL	(1.5-30nm)*100	0.0068	890	n	1.0×10^{18}
SnTe/PbSe SL	(1.5-20nm)*100	0.0052	780	n	1.5×10^{18}

PbTe/SnTe superlattices.⁶ These properties come from the type-II band structure. Figure 3 shows a schematic L-point subband structure for the superlattice. In the (111) growth, real subband structures are more complicated because there are two kinds of subbands corresponding to the valley with superlattice direction and other <111> valleys oblique to the superlattice direction. Solid lines show conduction-band-like subbands and dashed lines show valence-band-like subbands, and solid arrow indicates interband transition at PbSe band gap and dashed arrow shows electron transition from SnTe valence band to PbSe conduction band.

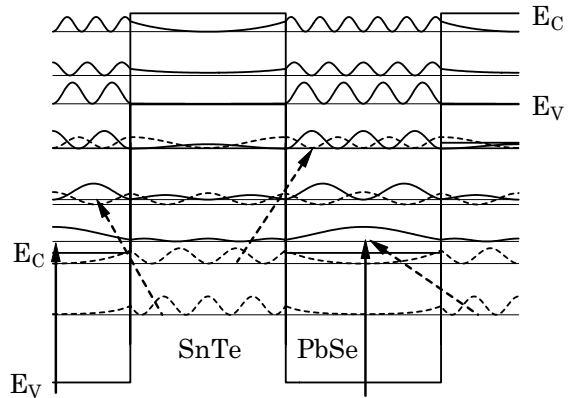


Fig.3. Subband structure and optical transitions in SnTe/PbSe superlattices.

valence band to PbSe conduction band. In the SnTe/PbSe superlattice with relatively thick SnTe and PbSe, the Hall coefficient becomes small owing to the coexistence of the electrons and holes with comparable numbers. The number of holes decreases with the decrease of SnTe layer thickness. Thus clear n-type conduction appeared for the superlattice with thin SnTe layer. In the superlattice, optical properties must be different from those of semiconductor film. Figure 4 shows the comparison of the optical transmission properties between the PbSe film and SnTe/PbSe superlattices. Solid lines and dashed lines show experimental and simulated spectra, respectively, and dashed-dotted lines show absorption coefficients

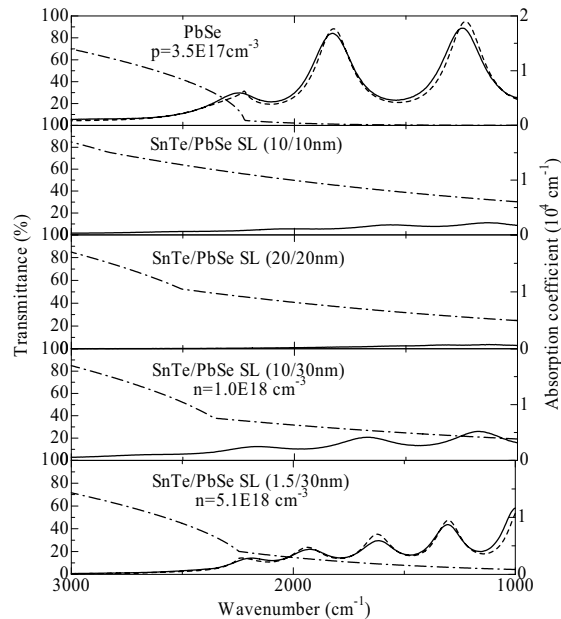


Fig.4 Optical transmission spectra of SnTe/PbSe type-II superlattices. Calculated absorption coefficients are shown by dashed-dotted lines.

show absorption coefficients

obtained by simulation. The simulation was performed only assuming the interband absorption and an exponential tail. The SnTe/PbSe superlattice indicated strong interband absorption over the band gap of PbSe (2200cm^{-1}). Furthermore, a strong absorption was also observed for the SnTe/PbSe superlattices over all spectral range below the band gap of PbSe. It is considered that the absorption comes from the electron transition inside SnTe valence band in the type-II superlattice, whose

tendency is different from the normal free carrier absorption proportional to the wavelength squared. Figure 5 shows the dependence of Seebeck coefficients on carrier concentration for the SnTe/PbSe superlattice. Negative value of the Seebeck coefficient corresponds to n-type conduction. Theoretical curves for PbSe were also indicated by solid line.⁷ The Seebeck coefficients of SnTe/PbSe superlattices were comparable with the theoretical values for PbSe.

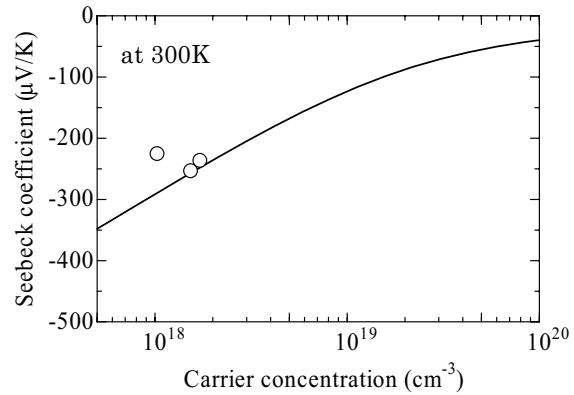


Fig.5. Seebeck coefficients of n-type SnTe/PbSe superlattices. Theoretical values for PbSe are indicated by solid line.

3. Conclusion

The SnTe/PbSe superlattices were prepared, and electrical properties were measured. The SnTe/PbSe superlattice with thin SnTe layer showed n-type conduction even though both SnTe and PbSe had p-type conduction, owing to type-II band offsets. Optical transmission properties of the SnTe/PbSe superlattice indicated semimetallic behavior. The Seebeck coefficients of the SnTe/PbSe superlattices were comparable with the theoretical values of PbSe.

References

- ¹ M. A. Tamor, H. Holloway, R. M. Ager, C. A. Gierczak, and R. O. Carter, *J. Appl. Phys.* **61**, 1094 (1987).
- ² K. Murase, S. Shimomura, S. Takaoka, A. Ishida, and H. Fujiyasu, *Superlattices and Microstructures* **1**, 177(1985).
- ³ A. Ishida, M. Aoki, and H. Fujiyasu *J. Appl. Phys.* **58** 1901 (1985).
- ⁴ S. Takaoka, T. Okumura, K. Murase, A. Ishida, and H. Fujiyasu *Solid State Commun.* **58**, 637 (1986)
- ⁵ A. Ishida, M. Aoki, H. Fujiyasu, *J. Appl. Phys.* **58**, 797 (1985).
- ⁶ E. I. Rogacheva, O. N. Nashchekina, A. V. Meriuts, S. G. Lyubchenko, M. S. Dresselhaus, and G. Dresselhaus, *Appl. Phys. Lett.* **86**, 063103 (2005).
- ⁷ Akihiro Ishida, Daoshe Cao, Sinsuke Morioka, Martin Veis, Yoku Inoue, and Takuji Kita, *Appl. Phys. Lett.* **92**, 182105 (2008).